PAPER

Flashing subdiffusive ratchets in viscoelastic media

To cite this article: Vasyl Kharchenko and Igor Goychuk 2012 *New J. Phys.* **14** 043042

New Journal of Physics
The open-access journal for physics

Flashing subdiffusive ratchets in viscoelastic media

Vasyl Kharchenko[1,2] **and Igor Goychuk**[1,3]

[1] Institute of Physics, University of Augsburg, Universitätstrasse 1, D-86135 Augsburg, Germany
[2] Institute of Applied Physics, 58 Petropavlovskaya Street, 40030 Sumy, Ukraine
E-mail: vasyl.kharchenko@physik.uni-augsburg.de and igor.goychuk@physik.uni-augsburg.de

New Journal of Physics **14** (2012) 043042 (21pp)
Received 24 January 2012
Published 27 April 2012
Online at http://www.njp.org/
doi:10.1088/1367-2630/14/4/043042

Abstract. We study subdiffusive ratchet transport in periodically and randomly flashing potentials. A central Brownian particle is elastically coupled to the surrounding auxiliary Brownian quasi-particles, which account for the influence of the viscoelastic environment. Similar to standard dynamical modeling of Brownian motion, the external force influences only the motion of the central particle, not affecting directly the environmental degrees of freedom. Just a handful of auxiliary Brownian particles suffices to model subdiffusion over many temporal decades. Time modulation of the potential violates the symmetry of thermal detailed balance and induces an anomalous subdiffusive current which exhibits a remarkably small dispersion at low temperatures, as well as a number of other surprising features such as saturation at low temperatures, and multiple inversions of the transport direction upon a change of the driving frequency in the non-adiabatic regime. It is shown that the subdiffusive current is finite at zero temperature for random flashing and can be finite for periodic flashing for a certain frequency window. Our study generalizes classical Brownian motors towards operating in sticky viscoelastic environments such as the cytosol of biological cells or dense polymer solutions.

[3] Author to whom any correspondence should be addressed.

Contents

1. Introduction

The physics of noise-assisted driven transport is currently a well-established area of research [1, 2]. Most papers are devoted to classical transport in neglecting non-Markovian and even inertial effects. The corresponding stochastic nonlinear dynamics can be described by a Langevin equation in time-dependent potentials and/or by the associated Fokker–Planck equation for the noise-averaged dynamics of the probability density of an ensemble of moving particles. Key ingredients are nonlinear dynamics in periodic potentials unbiased on average, friction and thermal noise related by the fluctuation–dissipation theorem (FDT) and an external driving which violates the symmetry of thermal detailed balance ensured by the FDT at thermal equilibrium. The emerged dissipative out-of-equilibrium directed transport is necessarily accompanied by entropy production and related heat dissipation.

A paradigmatic example is provided here by transport in flashing potentials [3], such as the one in figure 1. In a standard Markovian overdamped setup, when the potential is off, an initially localized particle diffuses with the position variance growing linearly, $\langle \delta x^2(t) \rangle \propto t$, which corresponds to normal diffusion. When the potential is on, the particle relaxes to a minimum of the potential and the probability distribution becomes at least bimodal with a larger peak corresponding to sliding down a less steep side of the potential (as a larger basin of attraction corresponds to a larger distance between the minimum and the maximum of a spatially asymmetric but periodic potential). When flashing repeats, either periodically or stochastically, but sufficiently slowly, the net transport is expected to emerge in the left, natural direction, with the averaged particle's position growing linearly in time. Such a normal transport is characterized by mean velocity. This natural direction is opposite to the one in the fluctuating tilt potential ratchets of the same potential form [4, 5]. For a fixed unbiased on average potential, the total heat exchange between the particle and its environment is zero, FDT holds, and directed transport is forbidden by the symmetry of thermal detailed balance. Out-of-equilibrium potential fluctuations violate this symmetry and induce directed transport. There emerges an overall uncompensated excess heat flow to the environment associated with the corresponding entropy production. A part of the energy put in the repeating potential flashing is dissipated as excess heat and another part can be used to do useful work against a load. If the load is absent all the consumed energy is dissipated as excess heat (futile motor) because the mechanical energy of

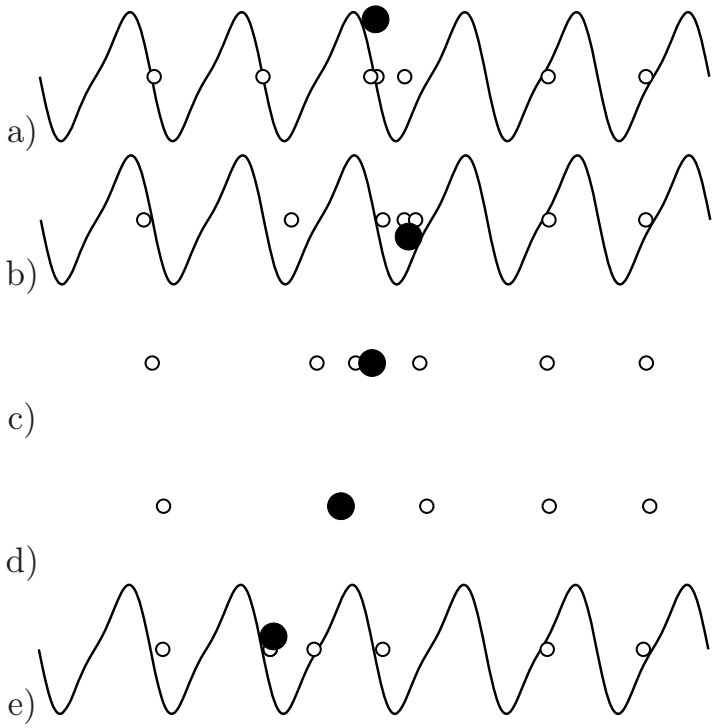

Figure 1. Snapshots of numerical simulations of the dynamics in equation (13) at different instants of time: (a) $t = 0.1$, (b) $t = 0.4$, (c) $t = 1.6$, (d) $t = 2.0$ and (e) $t = 2.5$. One Brownian particle (big filled circle) is coupled to auxiliary particles (small empty circles) at a temperature $T = 0.1$ and moves in the potential (15) periodical flashing with frequency $\nu = 1.0$ and amplitude $U_0 = 0.75$.

the motor particle remains on average unchanged. This is a well-established by now physical picture [6, 7]. This basic model explains, e.g., the operating of single-headed kinesin motors [8], where the energy to drive stochastic cycles is provided in effect by the energy of ATP hydrolysis.

Generalization of this approach to account for non-Markovian friction with memory is not trivial. The memory effects appear, e.g., due to viscoelasticity of the environment [9–15]. Even if a corresponding generalized Langevin equation (GLE) [16–19] is well known for any linear model of friction with memory, the corresponding non-Markovian Fokker–Planck equation (NMFPE) [20–24] remains simply unknown for general nonlinear force fields. The cases of constant force, or a linear in coordinate force, where the corresponding NMPPEs are known [20], are not useful in the present context. Particularly interesting is the case of a power-law decaying memory kernel [10] which corresponds to subdiffusion and is associated with the Cole–Cole dielectric response of viscoelastic media [25, 26]. Such viscoelastic subdiffusion has recently been found relevant also for transport in polymer networks [27, 28], cytosol of biological cells [29] and akin crowded fluids [30]. The corresponding fluctuating tilt or rocking ratchets in viscoelastic media have recently been proposed and studied in [31, 32] with a number of quite unexpected and surprising properties revealed. There is growing interest in the ratchet effect in glass-like environments [33]. Flashing ratchet transport in dynamically disordered potentials was proposed and studied earlier in [34]. Transport in disordered potentials is known

to be equivalent within the mean-field effective medium approximation to a continuous time random walk (CTRW) approach with independent residence times in traps [35–37]. This places our research into a general context of anomalous transport processes in complex media [35–38]. However, our approach to anomalous transport in viscoelastic media is very different from the one based on uncorrelated CTRW.

This work is devoted to flashing viscoelastic ratchets, which turn out to be no less interesting than the rocking viscoelastic ratchets of [31, 32], and we shall take advantage of the approach to anomalous subdiffusive transport developed recently in [14, 15, 31].

2. Dynamical approach to viscoelastic transport and stochastic modeling

We start with a well-established dynamical approach to the theory of Brownian motion [17, 19]. The environment is modeled by a set of N_0 particles with masses m_i harmonically coupled with the spring constants κ_i to the Brownian particle of mass m:

$$m\ddot{x} = f(x,t) - \sum_{i=1}^{N_0} \kappa_i (x - q_i), \tag{1}$$

$$m_i \ddot{q}_i = \kappa_i (x - q_i), \tag{2}$$

where q_i are the coordinates of the environmental particles, x is the coordinate of the Brownian particle and $f(x,t)$ is an external force which affects only the motion of the Brownian particle but not the environment. As is usual, using the Green function of the harmonic oscillator, one can express the bath oscillator coordinates $q_i(t)$ in equation (2) via the initial values $q_i(0)$ and $p_i(0)$ for arbitrary $x(t)$:

$$\begin{aligned} q_i(t) &= q_i(0)\cos(\omega_i t) + \frac{p_i(0)}{m_i\omega_i}\sin(\omega_i t) + \frac{\kappa_i}{m_i\omega_i}\int_0^t \sin[\omega_i(t-t')]x(t')\mathrm{d}t' \\ &= [q_i(0) - x(0)]\cos(\omega_i t) + \frac{p_i(0)}{m_i\omega_i}\sin(\omega_i t) + x(t) - \int_0^t \cos[\omega_i(t-t')]\dot{x}(t')\mathrm{d}t'. \end{aligned} \tag{3}$$

Here, $\omega_i = \sqrt{\kappa_i/m_i}$ are the bath oscillator frequencies and integration by parts has been used to obtain the second equality. By substituting (3) into (1), one immediately obtains

$$m\ddot{x} + \int_0^t \eta(t-t')\dot{x}(t')\mathrm{d}t' = f(x,t) + \xi(t), \tag{4}$$

where

$$\eta(t) = \sum_i \kappa_i \cos(\omega_i t) \tag{5}$$

and

$$\xi(t) = \sum_i \kappa_i \left([q_i(0) - x(0)]\cos(\omega_i t) + \frac{p_i(0)}{m_i\omega_i}\sin(\omega_i t) \right). \tag{6}$$

Equation (4) is still a purely dynamical equation of motion which is exact; the dynamics of irrelevant degrees of freedom is however excluded. For example, it describes a time-reversible

dynamics if the external field $f(x,t)$ does not violate the time-reversal symmetry[4]. Then the trajectories governed by equation (4) are also most obviously time-reversal symmetric (see [39] on this point from a stochastic perspective). This is contrary to a widespread misperception. The *statistical* irreversibility comes about on the level of a bunch of trajectories *averaged* over different initial realizations of $q_i(0)$, $p_i(0)$. The loss of information due to averaging or coarse-graining is a well-known source of irreversibility leading to the statistical description of dynamical systems (see, e.g., [41]). As a matter of fact, the dynamics described by equation (4) is just a projection of a high-dimensional Hamiltonian dynamics onto two-dimensional (x, p) phase subspace.

Furthermore, one proceeds as in a typical molecular dynamics setup. The initial positions $q_i(0)$ and momenta $p_i(0)$ of the environmental oscillators in equation (6) are sampled (this is the only non-dynamical element in the theory) from a canonical distribution at temperature T,

$$\rho(\{q_i(0),\, p_i(0)\}|x(0)) = \frac{1}{Z}\exp\left[-\frac{1}{2k_{\mathrm{B}}T}\sum_{i=1}^{N_0}\left(\frac{p_i^2(0)}{m_i}+\kappa_i[q_i(0)-x(0)]^2\right)\right], \tag{7}$$

conditioned on the initial position of the Brownian particle $x(0)$, where Z is the statistical sum of bath oscillators. Here one assumes that initial velocities of the bath oscillators are centered at zero, i.e. the medium is not moving as a whole. Likewise, the average $\langle q_i(0)\rangle = x(0)$, i.e. the medium is initially equilibrated adjusting to the Brownian particle localized at $x(0)$. The corresponding random force $\xi(t)$ becomes a stochastic process, which is obviously Gaussian and can be completely characterized by its first two statistical moments. The first moment is obviously zero, $\langle\xi(t)\rangle = 0$. Furthermore, with Gaussian averages $\langle p_i(0)p_j(0)\rangle = \delta_{ij}m_i k_{\mathrm{B}}T$, $\langle x_i(0)x_j(0)\rangle = \delta_{ij}k_{\mathrm{B}}T/\kappa_i$, $\langle x_i(0)p_j(0)\rangle = 0$, it is easy to show that

$$\langle\xi(t')\xi(t)\rangle = k_{\mathrm{B}}T\eta(|t-t'|) \tag{8}$$

for any set of bath oscillators. This is the celebrated fluctuation–dissipation relation, or the second FDT by Kubo [16]. The bath oscillators are conveniently characterized by the spectral density [19]

$$J(\omega) = \frac{\pi}{2}\sum_i \frac{\kappa_i^2}{m_i\omega_i}\delta(\omega-\omega_i) = \frac{\pi}{2}\sum_i m_i\omega_i^3\delta(\omega-\omega_i). \tag{9}$$

It allows one to express $\eta(t)$ as $\eta(t) = (2/\pi)\int_0^\infty \mathrm{d}\omega J(\omega)\cos(\omega t)/\omega$ and the noise spectral density as $S(\omega) = 2k_{\mathrm{B}}TJ(\omega)/\omega$ via the Wiener–Khinchin theorem, $S(\omega) = \int_{-\infty}^{\infty}\langle\xi(t)\xi(0)\rangle\,\mathrm{e}^{\mathrm{i}\omega t}\,\mathrm{d}t$. The choice $J(\omega) = \eta_\alpha|\sin(\pi\alpha/2)|\omega^\alpha$ with $0<\alpha<2$ yields the fractional Gaussian noise (fGn) $\xi(t)$ introduced by Mandelbrot and van Ness [42]. For $0<\alpha<1$ (sub-Ohmic thermal bath [19]),

$$\eta(t) = \eta_\alpha t^{-\alpha}/\,\Gamma(1-\alpha), \tag{10}$$

where $\Gamma(z)$ is a standard gamma function. This choice yields subdiffusion asymptotically, $\langle\delta x^2(t)\rangle \sim t^\alpha$, for an ensemble of particles [19]. The corresponding GLE (4) is also termed the fractional GLE or FLE [15, 24, 43, 44] with the use of the notion of fractional Caputo derivative to shorthand the frictional term, and the coefficient η_α is termed then the fractional

[4] Time-reversal symmetry can be *dynamically* broken by an external time-dependent field. For example, a harmonic mixing driving, $f(t) = A_1\cos(\Omega t) + A_2\cos(2\Omega t+\phi)$, does violate the time-reversal symmetry dynamically for $\phi \neq 0$ [40].

friction coefficient. Such a dynamical modeling requires a very large $N_0 \to \infty$ number of the bath oscillators with a quasi-dense spectrum. As a matter of fact, the non-Markovian stochastic process $[x(t), \dot{x}(t)]$ described by the GLE (4), (8) can mathematically be embedded as a component of a hyper-dimensional singular Markovian process described by the dynamical equations of motion with random initial preparations corresponding to different realizations of the process [45].

2.1. Stochastic modeling

One can drastically reduce the dimension of a Markovian embedding by using auxiliary stochastic variables instead of dynamical ones. Indeed, one can use just a handful of N auxiliary Brownian particles clouding around the central particle [15, 46] while modeling the rest as friction and noise acting on these representative ones. Such Brownian quasi-particles can serve to model sticky viscoelastic media. Then, one replaces dynamical equations (1) and (2) with stochastic ones [15, 46],

$$m\ddot{x} = f(x,t) - \sum_{i=1}^{N} k_i(x - x_i), \tag{11}$$

$$m_i\ddot{x}_i = k_i(x - x_i) - \eta_i\dot{x}_i + \sqrt{2\eta_i k_B T}\,\zeta_i(t), \tag{12}$$

where x_i are the coordinates of auxiliary particles, k_i are the corresponding coupling constants, $\sqrt{2\eta_i k_B T}\,\zeta_i(t)$ are thermal Gaussian forces, with zero range of correlation, $\langle \zeta_i(t)\zeta_j(t')\rangle = \delta_{ij}\delta(t-t')$, and η_i are the corresponding friction coefficients. Moreover, the overdamped limit for these auxiliary stochastic medium oscillators, $m_i \to 0$, yields

$$\begin{aligned} \dot{x} &= v, \\ m\dot{v} &= f(x,t) + \sum_{i=1}^{N} u_i(t), \\ \dot{u}_i &= -k_i v - \nu_i u_i + \sqrt{2\nu_i k_i k_B T}\,\zeta_i(t), \end{aligned} \tag{13}$$

where $\nu_i = k_i/\eta_i$ are the relaxation rates of the introduced viscoelastic forces $u_i = -k_i(x - x_i)$. The last equation for u_i is similar to Maxwell's relaxation equation for the viscoelastic force in the macroscopic theory of viscoelasticity [9], which is augmented by the corresponding Langevin force in accordance with FDR. Such a description was introduced in [14, 15, 31, 46] to model anomalous Brownian motion in complex viscoelastic media within a generalized Maxwell model. For the particular case of only one auxiliary particle (the Maxwell model of viscoelasticity), the earlier description in [47, 48] leading to GLE with thermal Ornstein–Uhlenbeck noise is readily reproduced. Excluding the dynamics of auxiliary variables $u_i(t)$ and assuming that initially forces $u_i(0)$ are thermally Gaussian-distributed with zero mean and dispersion $\langle u_i^2(0)\rangle = k_i k_B T$ yields again the GLE (4) with the corresponding memory kernel presented by a sum of exponentials,

$$\eta(t) = \sum_{i=1}^{N} k_i\, \mathrm{e}^{-\nu_i t}. \tag{14}$$

The corresponding noise $\xi(t)$ presents the sum of the Ornstein–Uhlenbeck noises.

The power-law memory kernel (10) can be reliably approximated by such a sum [14] over a large time interval $[t_l, t_h]$ by choosing $\nu_i = \nu_0/b^i$ and $k_i = C_\alpha(b)\eta_\alpha \nu_i^\alpha / \Gamma(1-\alpha)$. Here, $b > 1$ is a dilation (scaling) parameter and $C_\alpha(b)$ is a fitting dimensionless constant. The physical meaning of ν_0 is a high-frequency (short-time) cutoff of the stochastic process $\xi(t)$, $t_l = \nu_0^{-1}$. The low-frequency (long-time) cutoff corresponds to $t_h = b^{N-1}t_l$. Similar scaling and approximation to a power law are well known in the theory of anomalous relaxation [35, 49]. By adjusting b and N one can approximate the power law (10) by a sum of exponentials (14) over about $r = N \log_{10} b - 2$ time decades. In order to ensure that the FLE dynamics is correctly simulated over r' time decades, one has to approximate the memory kernel properly over a larger number of time decades (adding several more quasi-particles to be on the safe side). Given desired r', the appropriate values of N and b are found by a comparison of the exact FLE solutions with the simulated ones in the potential-free case and with the semi-analytical solutions of the corresponding GLE equation obtained by the inversion of the corresponding exact analytical solutions in the Laplace space [14]. Weak dependence of r on b and N ensures a very powerful and accurate numerical approach to the FLE dynamics. Just a handful of auxiliary particles can suffice for all practical purposes. Of course, such a Markovian approximate embedding of FLE is not unique [50]. However, it appeals by a clear physical interpretation. Recently, the set (13) was formally generalized to numerically integrate also superdiffusive FLE [51]. Moreover, this approach can be considered also as a totally independent of FLE approach to model subdiffusion and subdiffusive transport.

3. Flashing ratchets

To study flashing ratchet transport we take $f(x,t) = f_0(x)r(t)$. Here, $f_0(x) = -U'(x)$ is a deterministic force acting on the particle (Brownian motor) when a potential $U(x)$ is switched on. Furthermore, $r(t)$ switches on/off taking just two values, zero and one, $r(t) = \{1, 0\}$. For $U(x)$ we take a typical ratchet potential

$$U(x) = -U_0 \left[\sin\left(\frac{2\pi x}{L}\right) + \frac{1}{4}\sin\left(\frac{4\pi x}{L}\right) \right], \tag{15}$$

with amplitude U_0 and period L. For $r(t)$ two models are considered: periodic versus random switching. In the periodic case, $r(t) = 1/2\left[1 + \mathrm{sgn}(\sin(2\pi\nu t))\right]$, where $\mathrm{sgn}(\cdot)$ is the standard signum function and ν is the linear frequency of flashing. The first switching occurs at $t_I = 1/2\nu$ and the total number of switchings is $N_{sw} \equiv T_{tot}/t_I = 2\nu T_{tot}$, where T_{tot} is the total computation time, which is equal to $N_s\,\mathrm{d}t$; N_s is the total number of integration steps of equation (4) and $\mathrm{d}t$ is a time step. Finally, one can write $N_{sw} = 2\nu N_s\,\mathrm{d}t$. For random switching $r(t)$, we consider the model of the dichotomous Markovian process (DMP) with the probability $p = 2\nu\,\mathrm{d}t$ to switch within $\mathrm{d}t$. Such a DMP is symmetric with equal residence time distributions in two states, $\psi(\tau) = 2\nu\exp(-2\nu\tau)$. Here, 2ν is the transition rate from one state to another (and also inverse of the mean residence time in a state). The mean flashing frequency $\langle\nu\rangle$ is equal to ν, $\langle\nu\rangle = \nu$.

In all simulations, we scale the coordinate in units of L and time in units of $\tau_v = (m/\eta_\alpha)^{1/(2-\alpha)}$. It is assumed to be temperature independent in accordance with the underlying Hamiltonian model [17, 19]. This is a standard assumption made also in other ratchet models [1, 2]. Furthermore, energy is scaled in $E = L^2\eta_\alpha^{2/(2-\alpha)}/m^{\alpha/(2-\alpha)}$ and temperature $T = E/k_B$. In this work, we choose $\alpha = 0.5$ and $b = 10$, $C_{1/2}(10) = 1.3$, and use $\nu_0 = 100$, $N = 12$. Such

a set of parameters gives an excellent approximation to the FLE dynamics over at least ten time decades, until $t_{\max} = 10^8$. Similar to [14, 31] this was checked by a comparison of the numerical results with the exact analytical solution for the position variance obtained within GLE and FLE [16, 43] in the force-free case. The numerical errors due to the memory kernel approximation are negligible as compared with the overall statistical error in our stochastic simulations (several per cent); for details see [14]. As in [32], numerical solutions of stochastic differential equations were performed on the graphical processor units (GPUs)[5] with double precision using the stochastic Heun method. The use of GPU computing allowed us to parallelize and accelerate simulations by a factor of about 100, as compared with conventional CPU computing.

The viscoelastic dynamics in the flashing ratchet potential is schematically shown in figure 1 (and also in the accompanying video abstract). The auxiliary particles are placed on the level $U = 0$ and are not influenced by the potential. Initially, when the potential is switched on, the Brownian particle moves in the potential well (see snapshots a and b). When the potential is off (snapshots c and d) the Brownian particle 'freely' subdiffuses, interacting only with auxiliary particles. After the potential is switched on again, the Brownian particle moves into the next potential well (see snapshot e) with the net motion occurring in the negative direction. During such motion not all auxiliary particles immediately follow the Brownian particle. Some of them are at long distances from the Brownian particle and are essentially less mobile than the Brownian particle and its nearest environment because they have essentially larger friction coefficients than other auxiliary particles. Within our model, the weaker the coupling constant k_i of an auxiliary particle to the Brownian one, the larger the corresponding frictional coefficient η_i. These very sluggish particles create a slowly fluctuating quasi-elastic force (a temporal biasing force [14, 15]) acting on the central particle. To separate the slow u_{slow} and the fast u_{fast} viscoelastic forces created by N-auxiliary quasi-particles we compute the mean time of the transitions to the neighboring potential wells $\langle\tau\rangle$. Those N_f forces which relax fast with rates $\nu_i > \langle\tau\rangle^{-1}$ are regarded as the fast forces. The remaining $N - N_f$ slow components can be considered as parts of a quasi-elastic force. 'Quasi-elastic' it is on the time scale $\langle\tau\rangle$. In figure 2, we show the probability densities for the fast, slow and total viscoelastic forces for a periodically flashing ratchet at fixed U_0 and different values of the flashing frequency and temperature. These densities are obtained by making snapshots of $u_i(t)$ acting on a single central Brownian particle within the time interval $[1.0 \times 10^5, 1.1 \times 10^5]$. Here, $u_{\text{total}} = \sum_{i=1}^{N} u_i$, $u_{\text{fast}} = \sum_{i=1}^{N_f} u_i$ and $u_{\text{slow}} = \sum_{i=N_f+1}^{N} u_i$. One can see that the fast viscoelastic force u_{fast} is symmetrically distributed around zero for all the presented cases, see the top row in figure 2. This means that N_f fast auxiliary quasi-particles move on average together with the central Brownian particle, fluctuating around its mean position. The Brownian particle clouded by N_f fast particles reminds us conceptually of the polaron picture in condensed matter physics. In contrast, the slow quasi-elastic force u_{slow} is characterized by asymmetric distribution around zero (the middle row in figure 2). It is directed on average opposite to the direction of motion of the Brownian particle, which depends on the flashing frequency. The emergence of this biased retarding force reflects the long-time memory effects. When the transport particle attempts to run away from the current position, e.g. under the influence of the flashing potential force, the medium (due to the slow relaxing degrees of freedom) remembers where the particle was and attempts to pull it back. The action of this quasi-elastic force obstructs the motion by introducing

[5] See http://www.nvidia.com/object/cuda_home_new.html

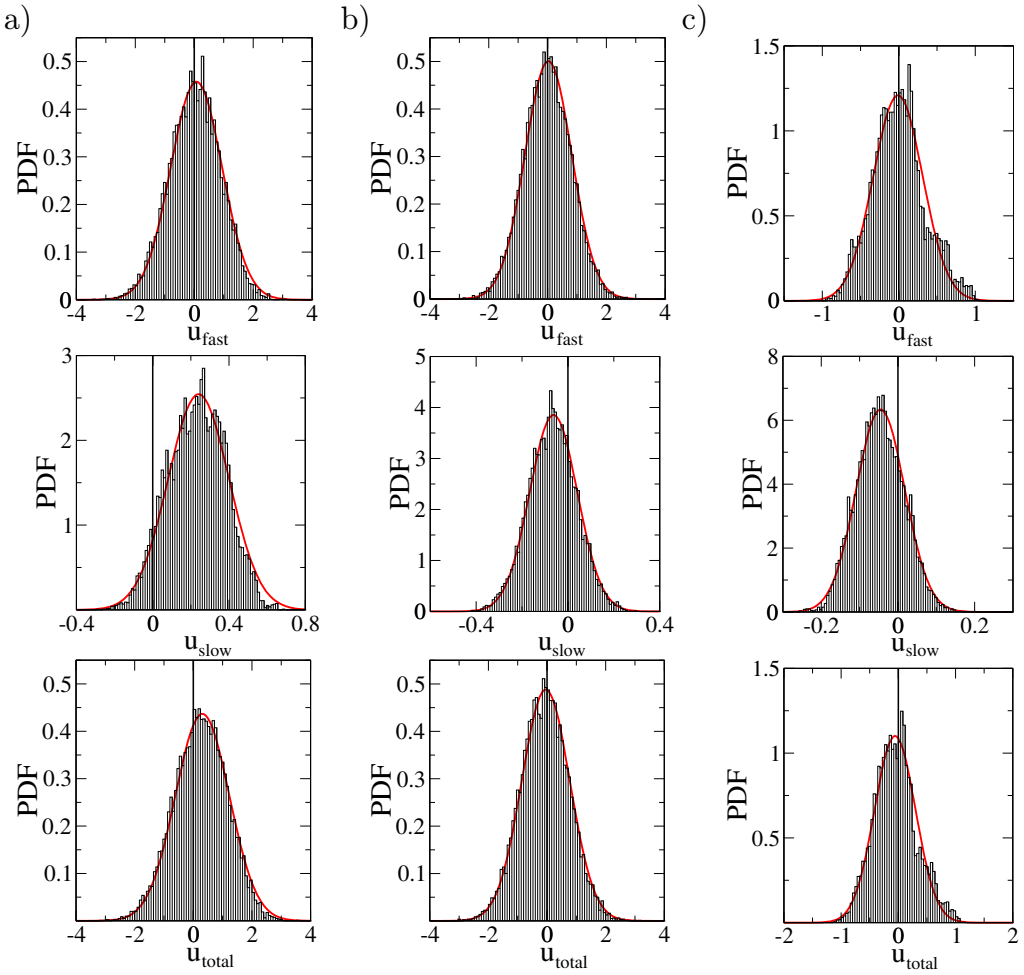

Figure 2. The probability density functions (PDFs) of the viscoelastic forces (fast u_{fast}, slow u_{slow} and total u_{total}, from the top to bottom, respectively) acting on the Brownian particle, as calculated on the time interval $[10^5, 1.1 \times 10^5]$ at $U_0 = 0.5$ for a periodically flashing ratchet: (a) $k_{\mathrm{B}}T = 0.05$ and $\nu = 0.75$; (b) $k_{\mathrm{B}}T = 0.05$ and $\nu = 0.375$; (c) $k_{\mathrm{B}}T = 0.0$ and $\nu = 0.375$. Full lines present Gaussian fits. $N_{\mathrm{f}} = 4$ in all cases.

negative correlations in the Brownian particle increments. It is the cause of the sub-diffusive character of the motion. As a result, the total viscoelastic force is biased against the net direction of motion. From figure 2 one can expect that a current inversion will occur with an increase of the flashing frequency ν. Moreover, figure 2(c) implies that the transport occurs also at zero temperature. These effects are studied below.

4. Results and discussion

In all simulations, we monitored two main statistical quantities: the mean position $\langle x(t)\rangle$ and the position variance $\langle \delta x^2(t)\rangle = \langle x^2(t)\rangle - \langle x(t)\rangle^2$. For the ensemble average, $N_{\mathrm{ens}} = 10^4$

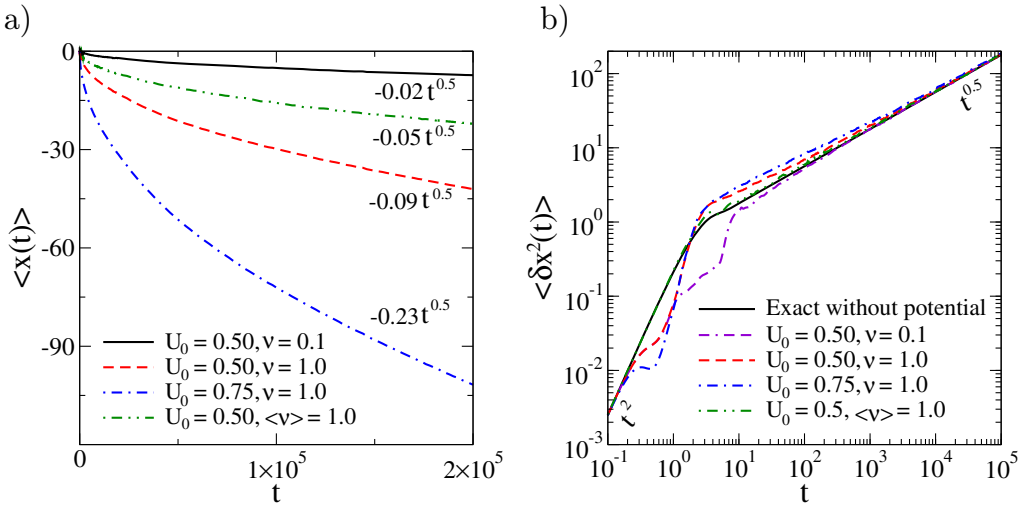

Figure 3. The mean particle position (a) and mean variance (b) at different values of the potential height U_0 and flashing frequency ν for periodic and random (green dash-dot-dot line) driving at $T = 0.25$. The black line in (b) depicts the exact analytical FLE result for the potential-free case.

trajectories were used. The focus is on such physical quantities as subdiffusive current (subvelocity) v_α, the subdiffusion coefficient D_α and the generalized Peclet number [31] $Pe_\alpha := v_\alpha L/D_\alpha = \lim_{t\to\infty} 2L\langle x(t)\rangle/\langle \delta x^2(t)\rangle$. The latter serves as a measure for the coherence and quality of anomalous stochastic transport, in analogy with Pe_1, introduced earlier for normal transport [52]. The subvelocity and the subdiffusion coefficient are defined as usual [15, 31, 37, 46]:

$$v_\alpha = \Gamma(1+\alpha) \lim_{t\to\infty} \frac{\langle x(t)\rangle}{t^\alpha}, \tag{16}$$

$$D_\alpha = \frac{1}{2}\Gamma(1+\alpha) \lim_{t\to\infty} \frac{\langle \delta x^2(t)\rangle}{t^\alpha}. \tag{17}$$

Here, the limit is understood in the following sense: t is large but still much smaller than the memory cutoff, which can always be made unreachable in numerical simulations and thus is irrelevant to the results presented. Practically, the values of v_α and D_α were calculated by fitting the numerical dependences $\langle x(t)\rangle$ and $\langle \delta x^2(t)\rangle$ with a power-law function $a_{\{v,D\}}t^\alpha$, extracting the corresponding a_v and a_D within the last time window of simulations. The total time of simulations was varied in the interval $[2\times 10^5, 10^6]$ depending on system parameters to guarantee a good fit with $\alpha = 0.5$ (convergence is slow); the time step was fixed at $\mathrm{d}t = 2\times 10^{-3}$.

Typical dependences for the mean particle position and variance on time for different values of the potential amplitude U_0 and flashing frequency ν are shown in figures 3(a) and (b), respectively. Here black solid, red dash and blue dash-dot lines correspond to periodic flashing, whereas the green dash-dot-dot line relates to the random case. The direction of transport in figure 3(a) is negative and the transport has a clearly subdiffusive character. We indicate in figure 3(a) also the corresponding power-law asymptotics. One can notice that stochastic flashing tends to delay the corresponding transport process in comparison with the periodic

one of the same frequency (cf red dash versus green dash-dot-dot lines), and the transport becomes faster with increasing flashing frequency (this is however not a universal feature, see below). The diffusion is initially always ballistic (universal regime), $\langle \delta x^2(t) \rangle = v_T^2 t^2$, where $v_T = \sqrt{k_B T/m}$ is the thermal velocity. This is because the Brownian particle's velocity is initially thermally distributed and the action of the medium requires some time to settle in. After some transient, subdiffusion follows asymptotically to one and the same universal dependence, $\langle \delta x^2(t) \rangle = 2D_\alpha t^\alpha / \Gamma(1+\alpha)$ with $D_\alpha = k_B T/\eta_\alpha$, as in the absence of potential, independently of the potential height and the presence of driving; cf figure 3(b). This universality (or a weak sensitivity in the case of a strong fast driving [31]) is a benchmark of viscoelastic subdiffusion [14, 15, 31, 46]. We elaborate on this fact below.

4.1. Ergodicity

An important issue in anomalous transport is ergodicity [53, 54], i.e. whether time average over a single-particle trajectory delivers a non-random result, the same for all identical particles, or whether principal randomness and scatter in the single-particle averages emerge. If this is the case, then the behavior and fate of each individual though identical particle are different, even in the limit of infinitely long trajectories, and only ensemble-averaging smears out this principal randomness and delivers a non-random result. In the case of ergodic transport, a single-trajectory average should coincide with the result of the ensemble averaging. For example, CTRW subdiffusion with divergent mean residence times in traps is patently non-ergodic [55] and single-trajectory averages obey some universal fluctuation laws [55–58] leading to a universal scaling relating such transport and diffusion in periodic potentials [59]. In contrast, viscoelastic subdiffusion, both free [60] and in time-independent potentials [14], was shown to be mostly ergodic, although some transient non-ergodic features can be present. Whether it remains ergodic also in time-fluctuating fields presents a nontrivial problem. First, we checked the asymptotic ergodicity of ratchet viscoelastic transport which is expected. To show that this is indeed the case, we plotted the fluctuating subvelocity $v_\alpha(t)$, obtained for a single trajectory as $v_\alpha(t) = \Gamma(1+\alpha)x(t)/t^\alpha$ in figure 4(a), versus the ensemble-average obtained with 10^4 particles. One can see that $v_\alpha(t)$ fluctuates around the ensemble average with the amplitude of fluctuations diminishing with t. In the limit $t \to \infty$ both the averages coincide and the transport is ergodic. For any finite t, statistical fluctuations are present, of course, also in the ergodic case. Next, a single-trajectory average of the squared displacement can be obtained as [14, 56, 57, 60]

$$\langle \delta x^2(t) \rangle_{\mathcal{T}} = \frac{1}{\mathcal{T}-t} \int_0^{\mathcal{T}-t} [x(t+t') - x(t')]^2 \, \mathrm{d}t'. \tag{18}$$

In the ergodic case, this average should coincide in the limit $\mathcal{T} \to \infty$ but for any t with the result of the ensemble averaging. If the agreement holds only for large t, then diffusion is asymptotically ergodic. For viscoelastic subdiffusion in fixed periodic potentials the agreement holds both for small t (ballistic regime) and for large t [14]. However, some deviations from ergodicity occur for intermediate t, on the time scale of diffusion over several potential periods. This is because even if the mean escape time exists the escape kinetics remains anomalous for activation barriers of an intermediate height [14].

Diffusional spreading derived from single trajectories is compared with the corresponding ensemble averages in figure 4(b). In the ballistic regime, using $x(t+t') - x(t') \approx v(t')t$ for small

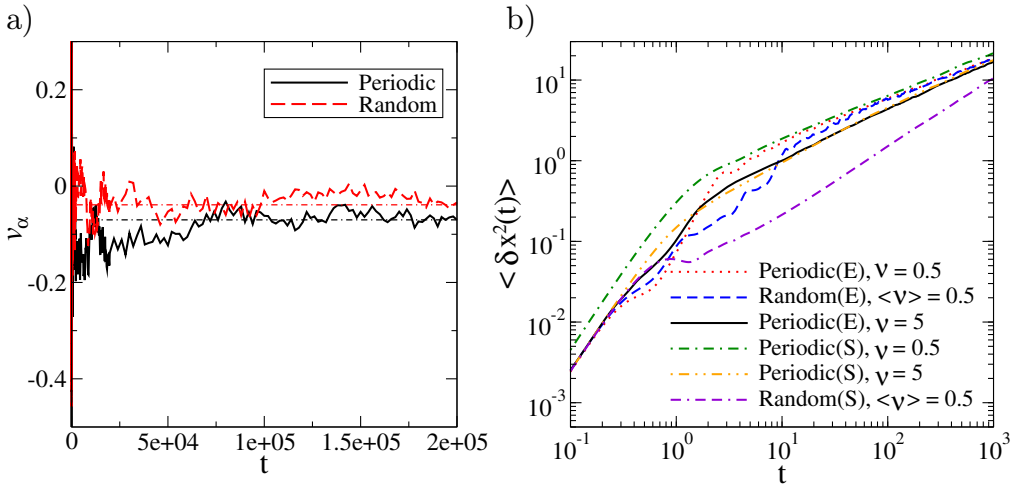

Figure 4. Subvelocity $v_\alpha(t)$, obtained for the single trajectory (a) for periodic and random flashing ratchets at $U_0 = 0.5$, $T = 0.25$ and linear frequency of flashing (its mean value) $\nu = 0.5$. The mean deviation $\langle \delta x^2(t) \rangle$ (b) for ensemble (E) and single trajectory (S) averaging at $U_0 = 0.5$ and $T = 0.25$ for periodic and random flashing ratchets. The time averaging for a single trajectory is done using 16-exponential approximation to memory kernel and $\mathcal{T} = 2 \times 10^7$.

t in equation (18), one obtains

$$\langle \delta x^2(t) \rangle_{\mathcal{T}} \approx t^2 \frac{1}{\mathcal{T} - t} \int_0^{\mathcal{T}-t} v^2(t')\, \mathrm{d}t' = \langle \delta v^2(t) \rangle_{\mathcal{T}} t^2. \tag{19}$$

Clearly, if in the limit $\mathcal{T} \to \infty$ the time average of $v^2(t)$ coincides with the ensemble average yielding v_{T}^2, then ergodicity holds also in the ballistic regime. In the absence of driving, this is indeed the case [14]. However, a periodic driving exciting coherent oscillations emerging due to a combined action of the external trapping potential and the viscoelastic cage effect can cause large additional temporal fluctuations in $v(t)$, which are not self-averaged in $\langle v^2(t) \rangle_{\mathcal{T}}$. Accordingly, such a periodically driven subdiffusion ceases to be ergodic in the ballistic regime. Temporally but on a large intermediate time scale, ergodicity is generally broken. Nevertheless, asymptotically it remains ergodic as figure 4(b) implies. Convergence to such an asymptotically ergodic regime is very slow. However, it improves with increased frequency of flashing; see the case $\nu = 5$ in figure 4(b). For random driving, ergodicity in the discussed sense holds also in the ballistic regime.

4.2. Frequency dependence

We proceed further with the dependence of the anomalous current v_α on frequency ν at a fixed value of temperature for different potential amplitudes U_0. In the case of fluctuating tilt subdiffusive ratchets [31], this dependence was especially intriguing: anomalous transport vanished in the limit of vanishing modulation frequency (adiabatic driving limit) and exhibited a maximum at intermediate frequencies. The origin of this maximum was related to the stochastic resonance effect in [32]. This is in sharp contrast to normal diffusion fluctuating tilt ratchets where transport optimizes, namely in the adiabatic limit. The results for periodic flashing

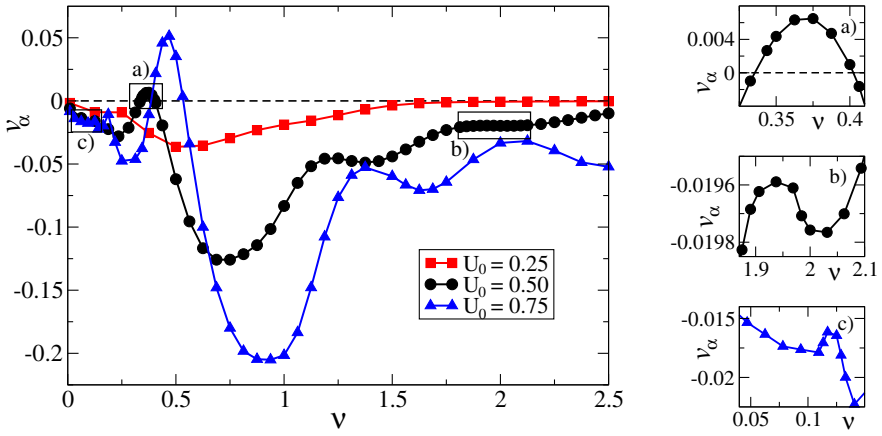

Figure 5. Anomalous current (subvelocity v_α) as a function of linear frequency of periodic flashing at a fixed temperature $T = 0.25$ for different values of U_0.

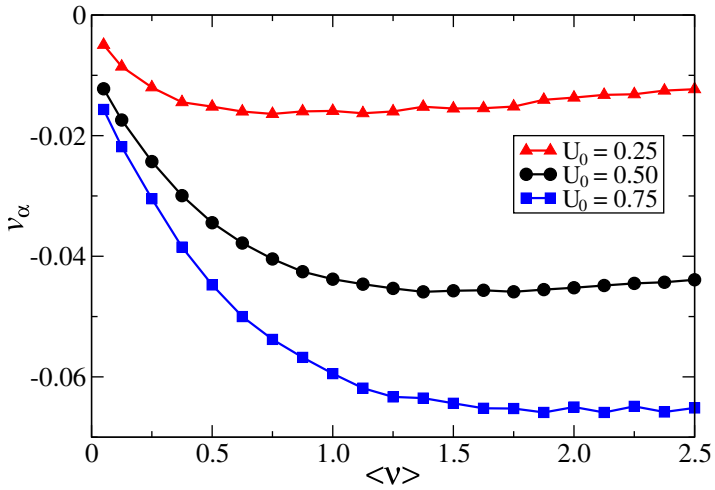

Figure 6. Anomalous current (subvelocity v_α) as a function of mean linear frequency of random flashing at a fixed temperature $T = 0.25$ for different values of U_0.

are shown in figure 5 and for stochastic driving in figure 6. For small driving frequencies subdiffusive transport occurs always in the natural negative direction, which is the opposite of the natural positive direction of the fluctuating tilt ratchet. Our anomalous Brownian motors share these features with their normal diffusion counterpart [1, 2]. There are, however, novel features that are due to the profound role of the inertial effects in our model. We recall that in the used scaling the unit of time corresponds to a scaling time constant τ_v of the decay of the velocity autocorrelation function. Correspondingly, the ballistic regime occurs until $t \sim 1$, when the potential is off. For a periodic driving at a small potential height $U_0 = 0.25 = T$ (see the red line with squares in figure 5), subvelocity takes negative values for all flashing frequencies considered. The dependence of $|v_\alpha|$ on ν has a unique maximum at $\nu_{c0} \simeq 0.5$, where subdiffusive transport is optimized, with negative v_α. For the fast-flashing regime, when $\nu > 1$ subvelocity

asymptotically decays to zero with ν. An increase in the ratchet potential height accompanied by an increased role of the inertial effects leads to a profound change in the character of the frequency dependence $v_\alpha(\nu)$ (see black curve with circles for $U_0 = 0.5$ in figure 5). Let us study this dependence in more detail. The first difference from the former case is a multiple (double) current inversion, realized around $\nu_{c1} \simeq 0.335$ and $\nu_{c2} \simeq 0.402$. An enlarged picture of this inversion effect is shown in the inset (a) placed on the right panel in figure 5. Here, a well-defined peak occurs at $\nu_{\max 1} = 0.375$ with positive values for $\nu_{c1} < \nu < \nu_{c2}$. Furthermore, on the left side of $\nu < \nu_{c1}$ there is a maximum of $|v_\alpha|$ for negative v_α. An increase of ν beyond ν_{c2} leads to a global maximum of $|v_\alpha|$ realized at $\nu_{\max 2} \simeq 0.75$. With further increase of flashing frequency, a complicated oscillatory pattern with several more relative minima and maxima in $|v_\alpha|$ emerges. With further increase of the potential amplitude these oscillatory resonance-like features become more pronounced—compare the two cases with $U_0 = 0.50$ and $U_0 = 0.75$ in figure 5. This is clearly related to the increased role of the inertial effects. Firstly, the amplitude of oscillations in $v_\alpha(\nu)$ increases. Secondly, many more extrema appear, see insets (b) and (c) in figure 5.

The optimal transport in the periodic flashing case (the maximal absolute value of subvelocity) is clearly related to a resonance effect, as figure 5 implies. To shed some light on this issue, let us calculate a characteristic frequency ω_d of damped oscillations at the bottom of potential (15) in harmonic approximation and compare the corresponding linear frequency $\nu_\mathrm{d} = \omega_\mathrm{d}/(2\pi)$ with optimal ν in figure 5 depending on the amplitude U_0. The undamped frequency of such oscillations is $\omega_0 = \sqrt{k/m}$, where $k = (\mathrm{d}^2U(x)/\mathrm{d}x^2)|_{x=x_{\min}} = U_0(2\pi/L)^2 3^{3/4}/\sqrt{2}$. Using GLE (4) for (10) and harmonic potential it is easy to show that the corresponding frequency ω_d can be found as the positive real root of the equation $\omega^2 + \gamma_\alpha \omega^\alpha = \omega_0^2$, where $\gamma_\alpha = \eta_\alpha/m$. From this in the used time scaling (through the anomalous time relaxation constant of the velocity autocorrelation function in the free-diffusion case), we obtain: $\nu_\mathrm{d} \approx 0.59$ for $U_0 = 0.25$, $\nu_\mathrm{d} \approx 0.86$ for $U_0 = 0.50$ and $\nu_\mathrm{d} \approx 1.07$ for $U_0 = 0.75$. In spite of the very crude character of the used approximation (the oscillations are clearly nonlinear), these values do semi-quantitatively agree with the corresponding optimal values $\nu_\mathrm{max} \approx 0.50$, $\nu_\mathrm{max} \approx 0.75$ and $\nu_\mathrm{max} \approx 0.94$ in figure 5. Importantly, they have the same tendency to increase with the potential amplitude U_0. Therefore, the maximal subvelocity in figure 5 seems to correspond to the case when the flashing synchronizes with the period of damped oscillations in the trapping potential. Moreover, the current inversion seems to occur when the flashing frequency is one half of the frequency of discussed oscillations reflecting a 2:1 synchronization. Indeed the peak of the inverted sub-current in figure 5 corresponds to $\nu_{\mathrm{r,max}} = 0.375$ for $U_0 = 0.50$ and $\nu_{\mathrm{r,max}} = 0.47$ for $U_0 = 0.75$. Other extrema are also clearly on the count of some resonance-like $n : m$ nonlinear stochastic synchronization effects (with n and m being some natural numbers reflecting the corresponding periods of driving and nonlinear intrawell oscillations, accordingly). Indeed, all the resonance peaks in figure 5 for $U_0 = 0.75$ (without inset) correspond consequently to 4:1, 2:1, 1:1, 2:3, 4:7 and 4:9 synchronizations. To shed more light on the detailed mechanism is, however, a very challenging problem which is far beyond the scope of the present work.

In the case of random flashing such resonances are absent. The corresponding dependences of anomalous current versus mean linear frequency $\langle\nu\rangle$ at a fixed temperature $T = 0.25$ for different values of U_0 are shown in figure 6. Here, contrary to the case of periodic flashing, one has simpler dependences $v_\alpha(\langle\nu\rangle)$ with one broad minimum for each considered potential amplitude U_0. An increase in U_0 leads to increases in the absolute values of subvelocity, broadening the minimum and shifting the minimum position towards larger values of the mean

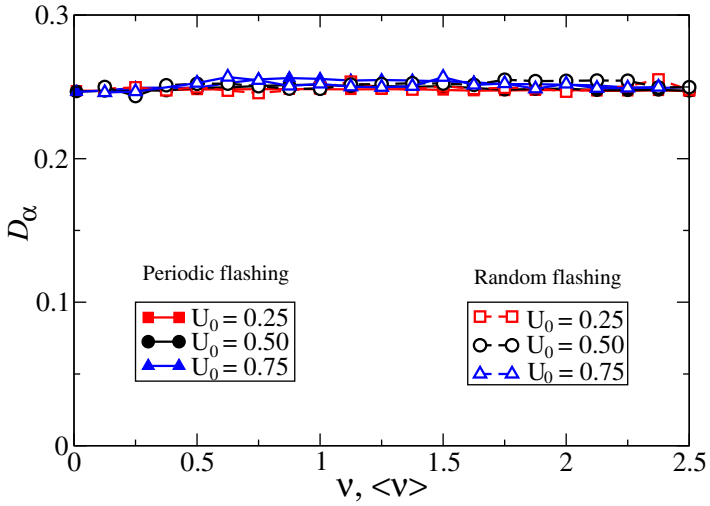

Figure 7. Sub-diffusion coefficient D_α as a function of linear frequency ν (or mean linear frequency $\langle\nu\rangle$) for periodic and random flashing, respectively, at a fixed temperature $T = 0.25$ and different values of U_0.

linear frequency. Thus, in the random flashing case the system is not manifestly sensitive to inertial effects due to the stochastic nature of flashing. The maximal value of subvelocity also becomes much smaller, compare figures 5 and 6, due to the absence of resonances.

A benchmark feature of viscoelastic subdiffusion is that it asymptotically does not depend on the presence of static periodic potential [14, 15, 46]. It was also only weakly dependent on driving in the case of rocking subdiffusive ratchets [31]. The diffusional spread in flashing ratchets is also practically not dependent on the potential amplitude U_0 and flashing frequency, as figure 7 illustrates. One can see that for both periodic and random flashing the anomalous diffusion coefficient does not display any profound dependence on the flashing frequency and the potential amplitude. It takes values around 0.25, which is $D_\alpha = T$ in the scaled units, with a deviation that is less than 3% and lies within the statistical error margin of our simulations. Therefore, the corresponding generalized Peclet number $Pe_\alpha := v_\alpha L/D_\alpha$, which measures the coherence and quality of transport, resembles the behavior of the absolute value of subcurrent in figures 5 and 6. In order to obtain Pe_α the absolute value of subcurrent $|v_\alpha|$ should be multiplied by factor 4.

4.3. Temperature dependence

The temperature dependence of subvelocity v_α and generalized Peclet number Pe_α is mostly intriguing, whereas the dependence of the subdiffusion coefficient D_α on temperature is expected to be trivial, $D_\alpha(T) = T$. We plotted numerical results for all three quantities in figure 8 (periodic flashing) and figure 9 (stochastic flashing) for three different test values of the flashing frequency, $\nu = 0.1$ (low-frequency), $\nu = 0.375$ (intermediate-frequency) and $\nu = 0.75$ (high-frequency). The temperature dependences of subvelocity share two common features; see figures 8(a) and 9(a). Firstly, the subvelocity is finite in the limit $T \to 0$ (this is always so for random flashing, but only for certain frequency windows in the case of periodic flashing). Secondly, it diminishes to zero in the limit of high temperatures. The latter is expected, but the

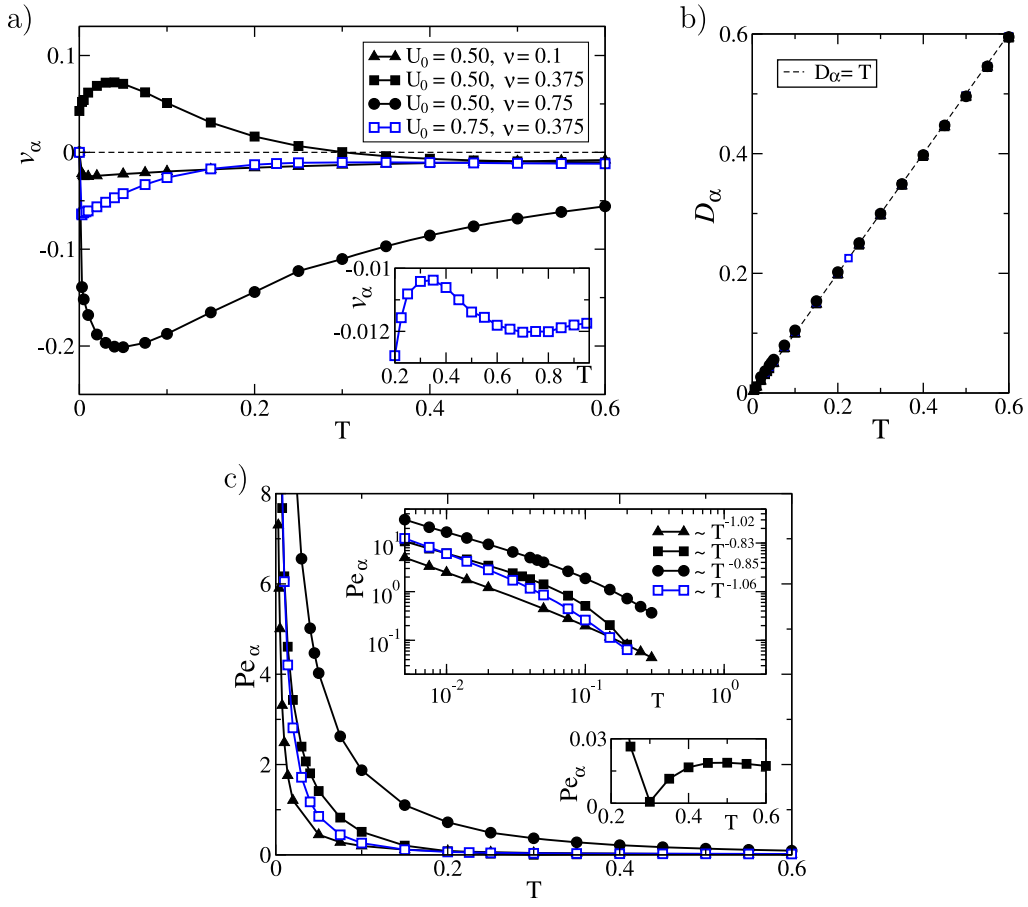

Figure 8. Anomalous current (subvelocity) v_α (a), subdiffusion coefficient D_α (b) and generalized Peclet number Pe_α (c) versus temperature for the periodic flashing ratchets at different values of the linear frequency of flashing ν and potential height U_0, as indicated in (a).

former is not, being highly surprising. Indeed, in a combination with the subdiffusion coefficient following the expected linear dependence and vanishing in the limit $T \to 0$ (see figures 8(b) and 9(b)), the nonzero value of v_α in this limit means that the basic mechanism of operation of our subdiffusive viscoelastic Brownian motors is very different from that in the case of normal overdamped Brownian motion.

Indeed, in the absence of viscoelastic effects the flashing Brownian motors of the studied kind are known to be essentially based on thermal diffusion, i.e. such transport is assisted by thermal fluctuations [8]. It is therefore expected to vanish in the limit $T \to 0$, where the thermal fluctuations vanish (neglecting of quantum effects). Our results show, however, that viscoelastic flashing ratchets are not based primarily on the thermal diffusion and thermal fluctuations. Because subdiffusion diminishes with decreasing temperature, the generalized Peclet number grows accordingly, $Pe_\alpha(T) \sim 1/T^\delta$ with δ in the range [0.83, 1.05]; see figures 8(c) and 9(c). Clearly, $Pe_\alpha \to \infty$ in the limit $T \to 0$, where the transport becomes perfect. These are long-range elastic correlations which are at work here in combination with inertial effects and the potential fluctuations. Namely, the external field acting on the Brownian particle changes

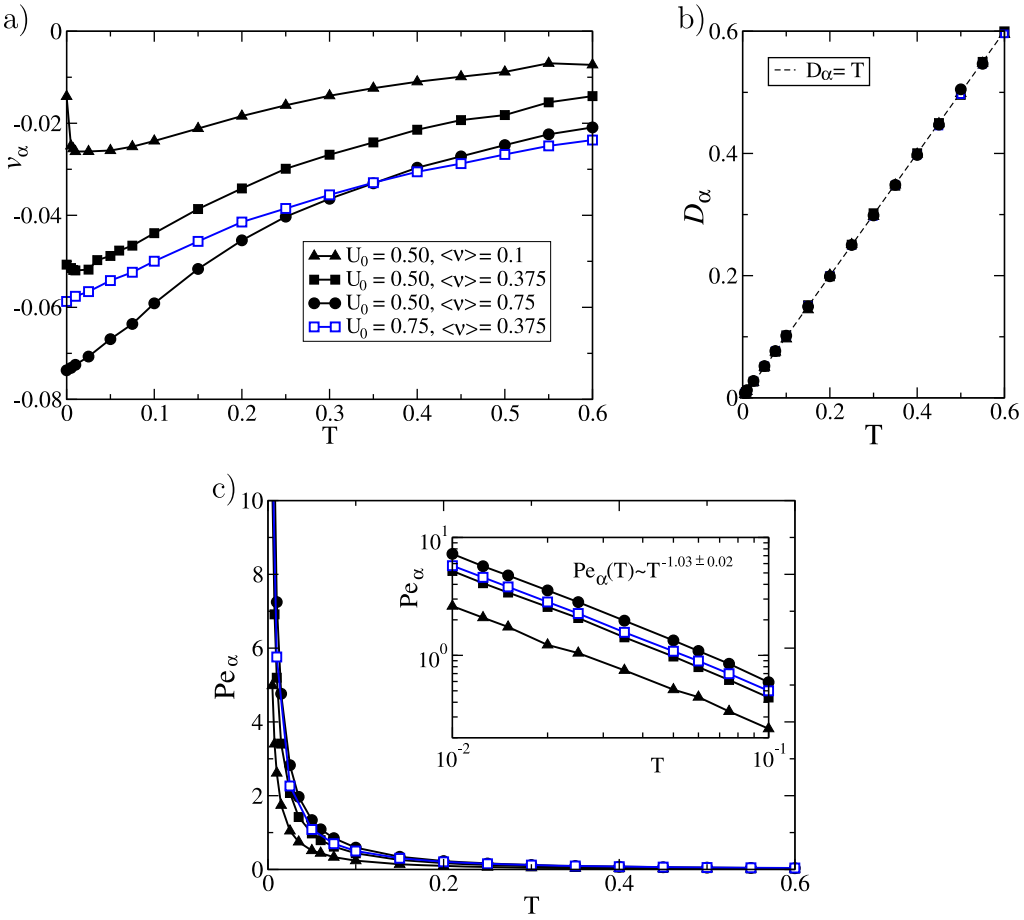

Figure 9. Anomalous current (subvelocity) v_α (a), subdiffusion coefficient D_α (b) and generalized Peclet number Pe_α (c) versus temperature for the random flashing ratchets at different values of the mean linear frequency of flashing $\langle\nu\rangle$ and potential height U_0, as indicated in (a).

abruptly (on–off process) the energy stored in the elastic springs. Not only the Brownian particle moves under the influence of $f_0(x)$, but also the auxiliary particles under the influence of Brownian particle. Some of them rapidly adjust their positions, but there are also slow particles which cannot follow immediately (see figure 2 and the corresponding discussion). Also the inertial effects become very important. This is why subdiffusive transport is generally not frozen even at $T = 0$ within our purely classical setup, where equation (13) corresponds to a periodically or randomly driven dynamical system. In order to clarify the origin of transport and the possible presence of chaotic diffusion at $T = 0$, we have simulated the corresponding dynamics by preparing initially all the Brownian particles with zero velocity (in correspondence to the Maxwell distribution at zero temperature) and uniformly distributing the central Brownian particles within a potential period. The corresponding ensemble averages are shown in figure 10 for both periodic and random flashing at $U_0 = 0.5$ and different values of the flashing frequency. The subdiffusive current is finite in figure 10(a). It increases with an increase of the mean frequency of random flashing (cf figure 9(a)). Sub-transport also occurs for certain frequencies of periodic flashing in accordance with figure 8(a). From equation (13) it follows that at $T = 0$

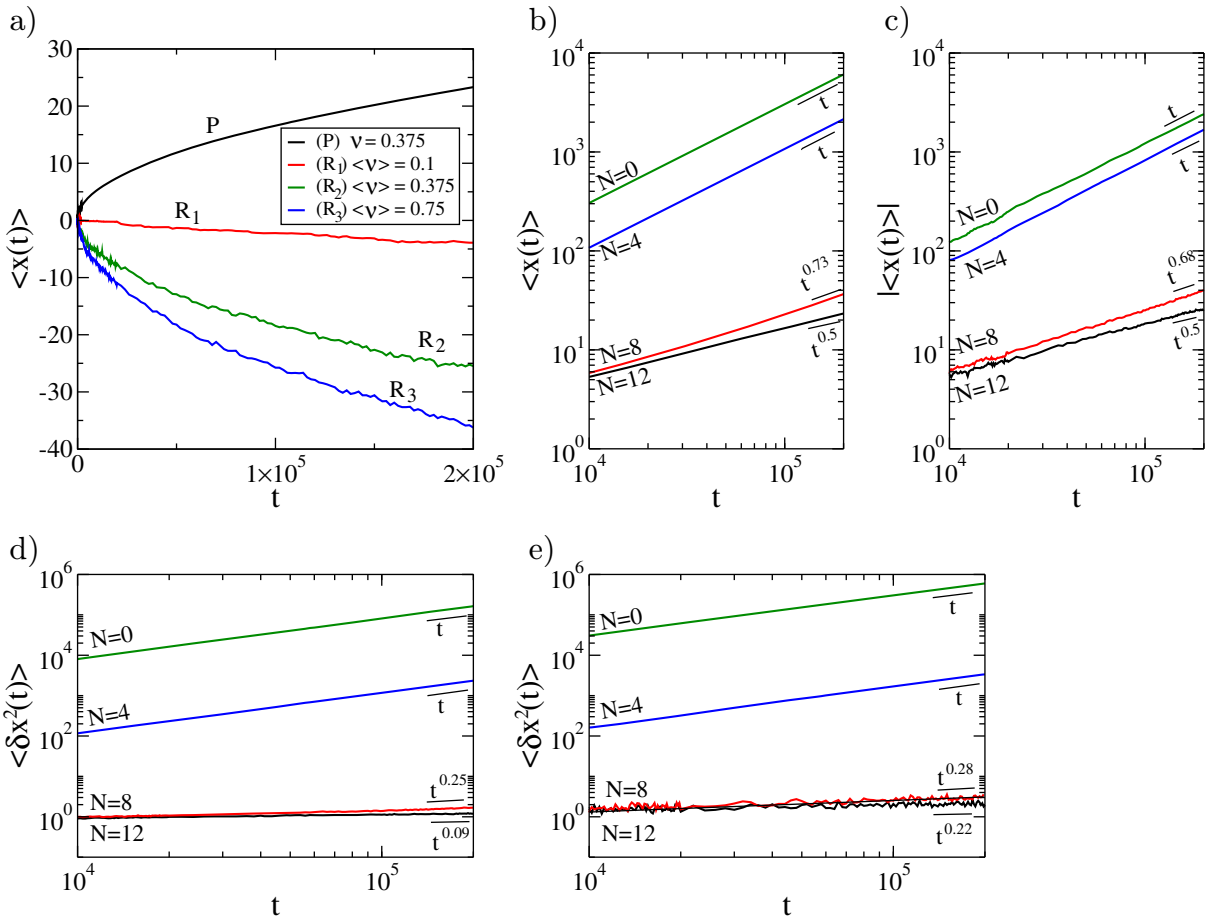

Figure 10. The mean particle position (a)–(c) and the variance (d), (e) at $T = 0$ and $U_0 = 0.5$: (a) for periodic and random flashing with several different flashing frequencies ν, $\langle\nu\rangle$ and $N = 12$; (b), (c) the mean particle position or its absolute value for different numbers N of auxiliary particles in the case of periodic and random flashing, $\nu = 0.375$ and $\langle\nu\rangle = 0.375$, respectively. (d), (e) The variance for periodic and random flashing, $\nu = 0.375$ and $\langle\nu\rangle = 0.375$, respectively.

the transport can be caused by viscoelastic and/or inertial effects only. As shown in figure 2 the fast quasi-particles move on average together with the Brownian particle, whereas the slow ones create a slowly fluctuating quasi-elastic force acting on the central particle in the direction opposite to the direction of motion. The action of this quasi-elastic force leads to subdiffusive transport. Therefore, one can expect that for a small number of auxiliary particles (without slow particles included) the transport will remain normal. To clarify this issue we used a different number of auxiliary particles N in our simulations depicted in figures 10(b) and (c), for a periodic driving with $\nu = 0.375$, and for a random driving with the same mean frequency, respectively. The case $N = 0$ corresponds to the memoryless dynamics where the only term u_1 remaining in the next simplest non-Markovian case $N = 1$ is replaced by $-\nu_1 v$ in equation (13), the second equation. It is seen that both in the periodic case (b) and in the random flashing case (c), the transport emerges at $T = 0$ without any viscoelastic effects. This is similar to the case studied in [61] for a different periodically flashing potential. Therefore,

the true origin of such normal transport lies in the inertial effects. The case $N = 1$ (the Maxwell model of viscoelasticity) coincides practically for the used parameters with the case $N = 0$ and for this reason it is not shown separately. The transport remains normal also in the case $N = 4$, where all the fast accompanying auxiliary particles are included. Remarkably, this normal zero-temperature transport is accompanied by normal diffusion of a chaotic origin (in the periodic driving case) as figures 10(d) (periodic flashing) and 10(e) (random flashing) demonstrate. The quality of the corresponding normal transport as measured by the Peclet number Pe_1 is, however, rather bad. The transport character is drastically changed upon inclusion of slow quasi-particles; see the cases $N = 8$ and $N = 12$ in figures 10(b)–(e). The case $N = 8$ is suitable for describing the sub-transport with $\alpha = 0.5$ only until a maximal time $t_{\max} = 10^4$. After this, a gradual transient to the asymptotically normal regime begins, as expected. In the case $N = 12$ such a normal regime (and even the onset of transition to it) is out of reach within a reasonable computational time, and the transport follows to the t^α law. Interestingly, the variance exhibits in both cases subdiffusion $\langle \delta x^2(t) \rangle \propto t^{\alpha_{\text{eff}}}$ with some α_{eff} which is much less than α. For this reason, the corresponding subdiffusion coefficient D_α is indeed zero, as defined by equation (17) and as figures 8(b) and 9(b) imply at $T = 0$. Differently from the normal one, the anomalously slow transport exhibits at $T = 0$ a superb quality with negligible dispersion ($Pe_\alpha \to \infty$) due to viscoelastic effects!

Generally, there are profound differences in the temperature dependence of anomalous transport in the cases of periodic and random flashing. So, in the case of periodic flashing the transport can occur in the counterintuitive positive direction; see the curve for $U_0 = 0.5$, $\nu = 0.375$ in figures 8(a) and 10(a). In this case, v_α remains finite also at $T = 0$, and an inversion of the current direction with increasing temperature is possible. This is not so for the other three curves in figure 8(a), where transport vanishes jump-like at $T = 0$. Therefore, it seems obvious that for periodic flashing there are frequency windows for permitted transport at $T = 0$. A detailed study of this interesting issue is beyond the scope of this paper and will be conducted elsewhere. In contrast, for random driving in figure 9(a), the transport remains always finite at $T = 0$. Moreover, here transport always occurs in the intuitive negative direction. Both in the random case and in the periodic case the transport can be optimized at some temperature $T_{\max} \neq 0$. It can be, however, also that $T_{\max} = 0$.

5. Conclusions

With this work, we put forward anomalously slow Brownian motors based on flashing subdiffusion in viscoelastic media. Both anomalous transport and subdiffusion were shown to be asymptotically ergodic. However, such a driven subdiffusion can be transiently non-ergodic on appreciably long time scales. The transport exhibits remarkably good quality at low temperatures, as characterized by the coherence of anomalous stochastic transport measured by the generalized Peclet number. Such transport does not vanish even at zero temperature in many cases (but not always in the case of periodic flashing) and is characterized by zero dispersion and diverging generalized Peclet number. In this limit, the transport is clearly induced by long-range elastic correlations in combination with inertial effects and potential flashing and not by the thermal noise of environment. This is surprising and at odds with a popular explanation of the origin of noise-induced flashing transport in the case of memory-free stochastic dynamics without inertial effects [1, 2]. Moreover, in the case of periodic driving the anomalous current exhibits multiple resonance-like features, can flow in the counterintuitive

direction and can invert its direction both with the change of flashing frequency and with the change of temperature. The inertial cage effects are essential for many observed features. In particular, they are crucial for the resonance-like features manifested for high potential barriers in the case of periodic flashing.

We hope that our research will stimulate further cross-fertilization of the field of fluctuation-induced transport and the field of anomalously slow transport and subdiffusion, which flourish at present with little interaction. There emerges increasing experimental support for the occurrence of subdiffusion in the cytoplasm of biological cells and we believe that there might also be room for operating sluggish molecular motors of the kind described.

Acknowledgments

Support from the Deutsche Forschungsgemeinschaft under grant number GO 2052/1-1 is gratefully acknowledged.

References

[1] Reimann P 2002 *Phys. Rep.* **361** 57
[2] Hänggi P and Marchesoni F 2009 *Rev. Mod. Phys.* **81** 387
[3] Ajdari A and Prost J 1992 *C. R. Acad. Sci. Paris* II **315** 1635
Astumian R D and Bier M 1994 *Phys. Rev. Lett.* **72** 1766
[4] Magnasco M O 1993 *Phys. Rev. Lett.* **71** 1477
[5] Bartussek R, Hänggi P and Kissner J G 1994 *Europhys. Lett.* **28** 459
[6] Jülicher F, Ajdari A and Prost J 1997 *Rev. Mod. Phys.* **69** 1269
[7] Astumian R D 1997 *Science* **276** 917
[8] Nelson P 2004 *Biological Physics: Energy, Information, Life* (New York: Freeman)
[9] Maxwell J C 1867 *Phil. Trans. R. Soc.* **157** 49
[10] Gemant A 1936 *Physics* **7** 311
[11] Mason T G and Weitz D A 1995 *Phys. Rev. Lett.* **74** 1250
[12] Jones R A L 2002 *Soft Condensed Matter* (Oxford: Oxford University Press)
[13] Waigh T A 2005 *Rep. Prog. Phys.* **68** 685
[14] Goychuk I 2009 *Phys. Rev.* E **80** 046125
[15] Goychuk I 2012 *Adv. Chem. Phys.* **150** 187
[16] Kubo R 1966 *Rep. Prog. Phys.* **29** 255
[17] Zwanzig R 1973 *J. Stat. Phys.* **9** 215
Zwanzig R 2001 *Nonequilibrium Statistical Mechanics* (Oxford: Oxford University Press)
[18] Coffey W T, Kalmykov Y P and Waldron J T 2004 *The Langevin Equation* 2nd edn (Singapore: World Scientific)
[19] Weiss U 1999 *Quantum Dissipative Systems* 2nd edn (Singapore: World Scientific)
[20] Adelman S A 1976 *J. Chem. Phys.* **64** 124
[21] Hänggi P, Thomas H, Grabert H and Talkner P 1978 *J. Stat. Phys.* **18** 155
[22] Hänggi P and Mojtabai F 1982 *Phys. Rev.* A **26** 1168
[23] Hynes J T 1986 *J. Phys. Chem.* **90** 3701
[24] Goychuk I and Hänggi P 2007 *Phys. Rev. Lett.* **99** 200601
[25] Cole K S and Cole R H 1941 *J. Chem. Phys.* **9** 341
[26] Goychuk I 2007 *Phys. Rev.* E **76** 040102
[27] Amblard F *et al* 1996 *Phys. Rev. Lett.* **77** 4470
[28] Caspi A, Granek R and Elbaum M 2002 *Phys. Rev.* E **66** 011916

[29] Guigas G, Kalla C and Weiss M 2007 *Biophys. J.* **93** 316
[30] Szymanski J and Weiss M 2009 *Phys. Rev. Lett.* **103** 038102
[31] Goychuk I 2010 *Chem. Phys.* **375** 450
[32] Goychuk I and Kharchenko V 2011 arXiv:1111.4833 [cond-mat.stat-mech]
[33] Giacomo G *et al* 2010 *J. Stat. Mech.* **L12002**
[34] Harms T and Lipowsky R 1997 *Phys. Rev. Lett.* **79** 2895
[35] Hughes B D 1995 *Random Walks and Random Environments* vols 1, 2 (Oxford: Clarendon)
[36] Bouchaud J-P and Georges A 1990 *Phys. Rep.* **195** 127
[37] Metzler R and Klafter J 2000 *Phys. Rep.* **339** 1
[38] Klafter J, Lim S C and Metzler R (ed) 2011 *Fractional Dynamics: Recent Advances* (Singapore: World Scientific)
[39] Hänggi P and Ingold G-L 2005 *Chaos* **15** 026105
[40] Goychuk I and Hänggi P 2000 *Stochastic Processes in Physics, Chemistry and Biology (Lecture Notes in Physics* vol 557*)* ed J A Freund and Th Pöschel (Berlin: Springer) pp 7–20
[41] Isihara A 1971 *Statistical Physics* (New York: Academic)
[42] Mandelbrot B B and van Ness J W 1968 *SIAM Rev.* **10** 422
[43] Lutz E 2001 *Phys. Rev.* E **64** 051106
[44] Burov S and Barkai E 2008 *Phys. Rev. Lett.* **100** 070601
[45] van Kampen N G 1992 *Stochastic Processes in Physics and Chemistry* 2nd, enlarged and extended edn (Amsterdam: North-Holland)
[46] Goychuk I and Hänggi P 2011 *Fractional Dynamics: Recent Advances* ed J Klafter *et al* (Singapore: World Scientific) chapter 13 pp 307–29
[47] Marchesoni F and Grigolini P 1983 *J. Chem. Phys.* **78** 6287
[48] Straub J E, Borkovec M and Berne B J 1986 *J. Chem. Phys.* **84** 1788
[49] Palmer R G, Stein D L, Abrahams E and Anderson P W 1984 *Phys. Rev. Lett.* **53** 958
[50] Kupferman R 2004 *J. Stat. Phys.* **114** 291
[51] Siegle P, Goychuk I and Hänggi P 2011 *Europhys. Lett.* **93** 20002
[52] Lindner B, Kostur M and Schimansky-Geier L 2001 *Fluct. Noise Lett.* **1** R25
[53] Yaglom A M 1972 *An Introduction to the Theory of Stationary Random Functions* (New York: Dover) (see section 1.4)
[54] Papoulis A 1965 *Probability, Random Variables, and Stochastic Processes* (New York: McGraw-Hill) see section 9-8, pp 323–35
[55] Bel G and Barkai E 2005 *Phys. Rev. Lett.* **94** 240602
[56] He Y, Burov S, Metzler R and Barkai E 2008 *Phys. Rev. Lett.* **101** 058101
[57] Lubelski A, Sokolov I M and Klafter J 2008 *Phys. Rev. Lett.* **100** 250602
[58] Sokolov I M, Heinsalu E, Hänggi P and Goychuk I 2009 *Europhys. Lett.* **86** 30009
[59] Goychuk I, Heinsalu E, Patriarca M, Schmid G and Hänggi P 2006 *Phys. Rev.* E **73** R020101
Heinsalu E, Patriarca M, Goychuk I, Schmid G and Hänggi P 2006 *Phys. Rev.* E **73** 046133
[60] Deng W H and Barkai E 2009 *Phys. Rev.* E **79** 011112
[61] Chen H, Wang Q and Zheng Z 2005 *Phys. Rev.* E **71** 031102